Impact of macromonomer molar mass and feed composition on branch distributions in model graft copolymerizations

Aristotelis Zografos,[†] Nathaniel A. Lynd,[‡] Frank S. Bates,*[,†] Marc A. Hillmyer[#,*]

[†]Department of Chemical Engineering and Materials Science, University of Minnesota, Minneapolis, MN, 55455-0132

[‡]McKetta Department of Chemical Engineering, The University of Texas at Austin, Austin, TX, 78712-1589

[#]Department of Chemistry, University of Minnesota, Minneapolis, MN, 55455-0431

*Corresponding authors (e-mail addresses: bates001@umn.edu; hillmyer@umn.edu)

Abstract

Graft polymers are useful in a versatile range of material applications. Understanding how changes to the grafted architecture, such as the grafting density (z), the side-chain degree of polymerization (N_{sc}), and the backbone degree of polymerization (N_{bb}), affect polymer properties is critical for accurately tuning material performance. For graft-through copolymerizations, changes to N_{sc} and z are controlled by the macromonomer degree of polymerization (N_{MM}) and initial fraction of the macromonomer in the feed (f_{MM}^0), respectively. We show that changes to these parameters can influence the copolymerization reactivity ratios and, in turn, impact the side-chain distribution along a graft polymer backbone. Poly((±)-lactide) macromonomers with N_{MM} values as low as *ca.* 1 and as high as 72 were copolymerized with a small-molecule dimethyl ester norbornene comonomer over a range of f_{MM}^0 values ($0.1 \leq f_{MM}^0 \leq 0.8$) using ring opening metathesis polymerization (ROMP). Monomer conversion was determined using ^{1}H nuclear magnetic resonance spectroscopy, and the data were fit using terminal and non-terminal copolymerization models. The results from this work provide essential information for manipulating N_{sc} and z, while maintaining synthetic control over the side-chain distribution for graft-through copolymerizations.

TOC graphic

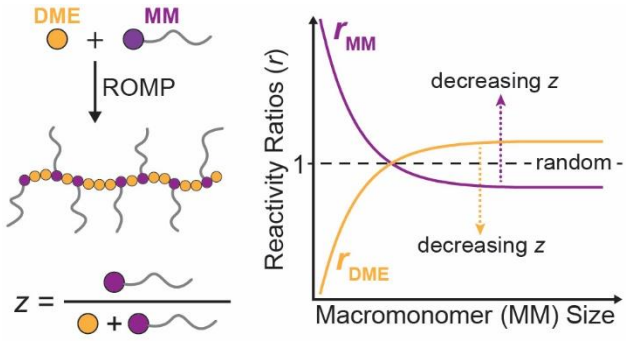
DME
MM
ROMP
z =
Reactivity Ratios (r)
r MM
r DME
1
decreasing z
decreasing z
random
Macromonomer (MM) Size

Compared to a linear polymer, the increased molecular complexity associated with grafted polymer architectures enables a broader range of accessible material properties. Whereas the description of a linear homopolymer requires a single degree of polymerization (N), a graft polymer requires three: The degree of polymerization of the side-chains (N_{sc}), the degree of polymerization of the backbone (N_{bb}), and the degree of polymerization between grafts (N_g). For random graft distributions, the latter is inversely related to a commonly used descriptor called the grafting density (z); z is defined as the average number of side-chains per backbone repeat unit. Tuning these parameters has been demonstrated to impact mechanical properties,[1,2,3,4,5,6] linear and non-linear melt flow behavior,[7,8,9,10,11,12] and self-assembly in graft copolymers.[13,14,15,16] Careful architectural changes can be leveraged to decouple material properties that are inextricably linked for linear polymers, such as molar mass and viscosity.[7]

Centrally important to graft polymer design is understanding how z impacts material performance.[7,12,14,15,17,18] Changing this parameter involves incorporating a small monomer diluent along the backbone through copolymerization with either a macromonomer (i.e., graft-through) or a small comonomer that side-chains can be grafted-to or grafted-from. Tuning the initial monomer feed composition provides control over the number density of side-chains (i.e., z), but not necessarily sequence. The sequence distribution (e.g., gradient, block, random) is controlled through the copolymerization reactivity ratios. Changes to this distribution will impact how graft polymers fill space and entangle,[19,20,21] which is relevant for understanding material behavior. Several synthetic methods (e.g., ring-opening metathesis,[22,23,24] anionic,[25] and controlled radical polymerizations[26,27,28,29,30]) have been employed to control the reactivity ratios in *graft-through* copolymerizations. Early work by Radke and Müller demonstrated that changes to the initial macromonomer feed composition ($f_{MM}^0 < 0.1$) can substantially affect the reactivity ratios, which was postulated to be due to changes to the density of chain segments near a propagating chain-end as f_{MM}^0 was varied. [30] Recently, Ren et al. demonstrated a similar effect for $f_{MM}^0 > 0.1$ in graft-through ring-opening metathesis copolymerizations (ROMP), though a significant assumption was

required for the analysis and no discussion of the reactivity ratios was provided.[24] In each case, the relation to the macromonomer's size was not investigated. These findings are particularly surprising, given that the reactivity ratios are traditionally understood to be independent of the initial monomer feed. For the *homopolymerization* of a macromonomer, several studies demonstrated the monomer reactivity to *decrease* to an asymptotic limit as its molar mass increased.[24,31] Contrary to these results, in *copolymerizations* of a macromonomer with a small comonomer, the macromonomer reactivity has been shown to *increase* as its molar mass increases[30] or, in another instance, shown to be *independent* of its molar mass.[25] These differences support the notion that trends in homopolymerizations do not necessarily dictate those for copolymerizations, where a comonomer can appear to be more or less reactive than indicated by its homopolymerization rate constant. For graft-through copolymerizations using ROMP, the effect that macromonomer size has on the reactivity ratios has not been studied. Also not well understood is how the reactivity ratio dependence on f_{MM}^0 is influenced by the macromonomer molar mass. If the observations in the literature are valid, this dependence should diminish as the macromonomer approaches its monomeric limit (i.e., $N_{sc} = 1$), since the reactivity ratios should not vary with the initial monomer feed for small molecule copolymerizations. To establish accurate structure-property relationships, it is important to understand how changing each of these parameters impacts the copolymerization kinetics. In this work we explore how N_{sc} and f_{MM}^0 influence the comonomer reactivity ratios in ROMP graft-through copolymerizations. Furthermore, we probe the ideality of ROMP copolymerizations by comparing the results from terminal and non-terminal models to establish the most suitable approach for fitting copolymerization kinetic data.

ROMP was used to synthesize a library of graft copolymers with varying N_{sc} and z (Scheme 1).

Scheme 1. Graft-through ROMP of a macromonomer (MM) and dimethyl ester comonomer (DME) using a Grubbs Generation III (G3) catalyst. Poly((±)-lactide) macromonomers with different degrees of polymerization ($N_{MM} = N_{sc}$) were used, where the acetylated norbornene approximates $N_{sc} \approx 1$. The DME concentration was adjusted to tune the grafting density (z) and initial macromonomer feed composition (f_{MM}^0), which also affected the backbone degree of polymerization (N_{bb}) through the equation shown for full monomer conversion.

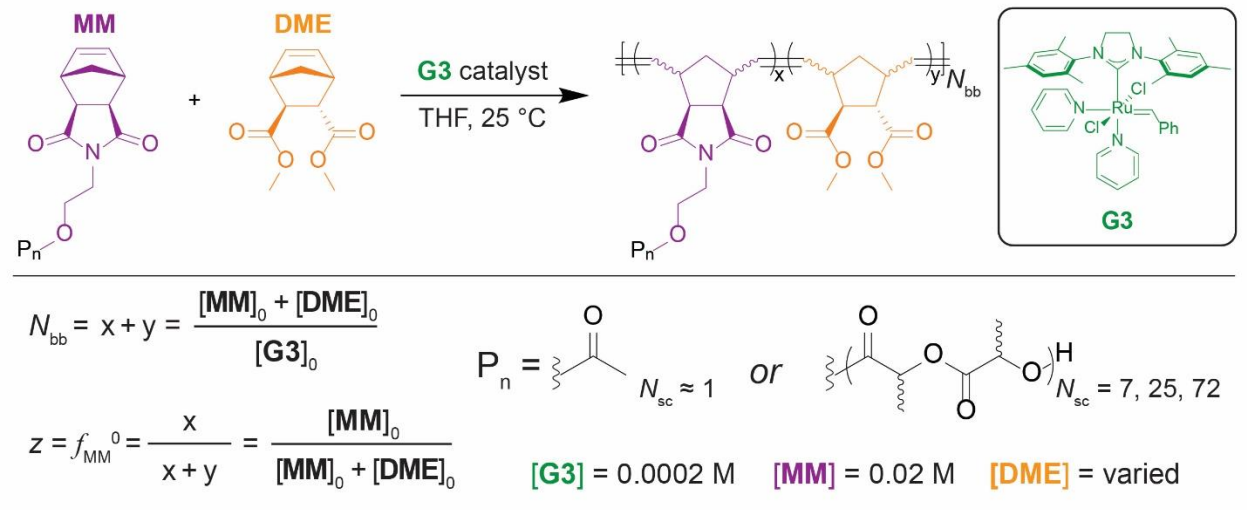

Poly((±)-lactide) macromonomers (MM) were copolymerized with a dimethyl ester comonomer (DME). Each macromonomer had a low dispersity ($Đ \leq 1.03$). Homopolymerizations of the macromonomers consistently gave high conversions (≥ 96%, Table S2, S3, S4), indicating a high degree of norbornene macromonomer end-group functionality. The macromonomer degree of polymerization ranged from $1 \leq N_{sc} \leq 72$. An acetylated norbornene molecule was used to approximate the monomeric limit of a single lactide repeat unit (i.e., $N_{sc} \approx 1$; for consistency and simplicity, the acetylated norbornene monomer will still be referred to as a "macromonomer"). As all copolymerizations were nearly complete within a few minutes, aliquots of the reaction were quenched at various times using methods described in the Supporting Information (Section 3.1). Grafting densities (z) between 0.1 and 0.8 were studied, which was accomplished by varying $f_{MM}^0 = 1 - f_{DME}^0$; $z = 0.5$ was not included to avoid numerical instabilities encountered with the kinetic models, as explained in the Supporting Information (Section 3.4). Assuming full monomer

conversion, z and f_{MM}^0 are equivalent. To tune the feed compositions, the initial DME concentration was varied while maintaining a constant initial MM and G3 concentration ($[MM]_0/[G3]_0 = 100$, Scheme 1). This approach minimized the number of variables between each copolymerization and avoided changes to the MM conversion, which has been shown to decrease for $[MM]_0/[G3]_0 > 100$.[32] The MM reactivity has also been demonstrated to decrease as $[MM]_0$ decreases.[33] Here, $[MM]_0$ was fixed to avoid this effect, enabling us to develop a clear understanding of the reactivity ratio dependence on N_{sc} and f_{MM}^0. Since the number of side-chains per graft polymer (n_a) is controlled by $n_a = [MM]_0/[G3]_0$, n_a was held constant. To decrease z, more of the small DME comonomer was added to the feed mixture, resulting in an increase in molar mass, which was confirmed by size exclusion chromatography (Figures 1, S10, S11, S12). Detailed information regarding the synthesis, as well as molecular characterization of the monomers and polymers, can be found in the Supporting Information (Section 2).

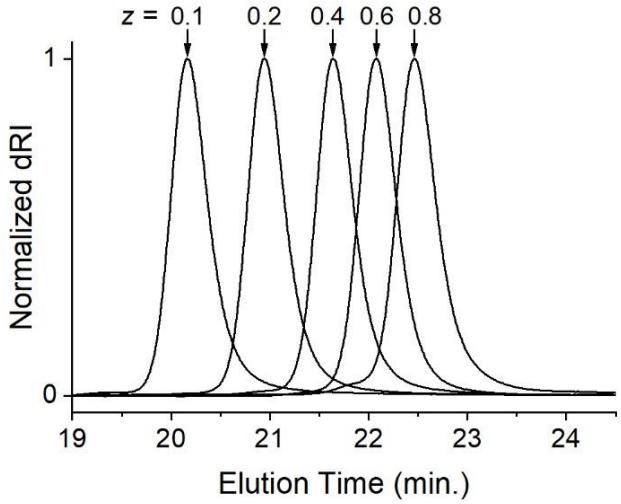

Figure 1. Representative size exclusion chromatography data for copolymers synthesized using the acetylated macromonomer ($N_{sc} \approx 1$) with DME as the comonomer. All polymers were characterized by low dispersity values ($Đ < 1.1$).

Non-terminal and terminal copolymerization models (Figures S16 and S17) were used to analyze monomer conversion, which was determined using ^{1}H NMR spectroscopy. Non-terminal fitting was accomplished using equations developed by Beckingham, Sanoja, and Lynd (BSL),[34]

whereas terminal fits were analyzed using an approach from Meyer and Lowry (ML).[35,36] Each of the equations are integrated forms of the respective copolymerization models and are not limited by the constraint of low monomer conversion associated with typical copolymer kinetic analyses. Furthermore, each approach enables both reactivity ratios to be determined from a single copolymerization reaction. Other approaches used in the literature (e.g., Jaacks equation, methods using the copolymerization equation, numerical solutions to the terminal model) require multiple reactions to determine all reactivity ratios.[22,36,37] The fitted conversion data used to determine all reactivity ratios can be found in the Supporting Information (Figures S18-S39).

Terminal and non-terminal models were compared for copolymerizations using macromonomers with $N_{sc} \approx 1$ (Figure 2A).

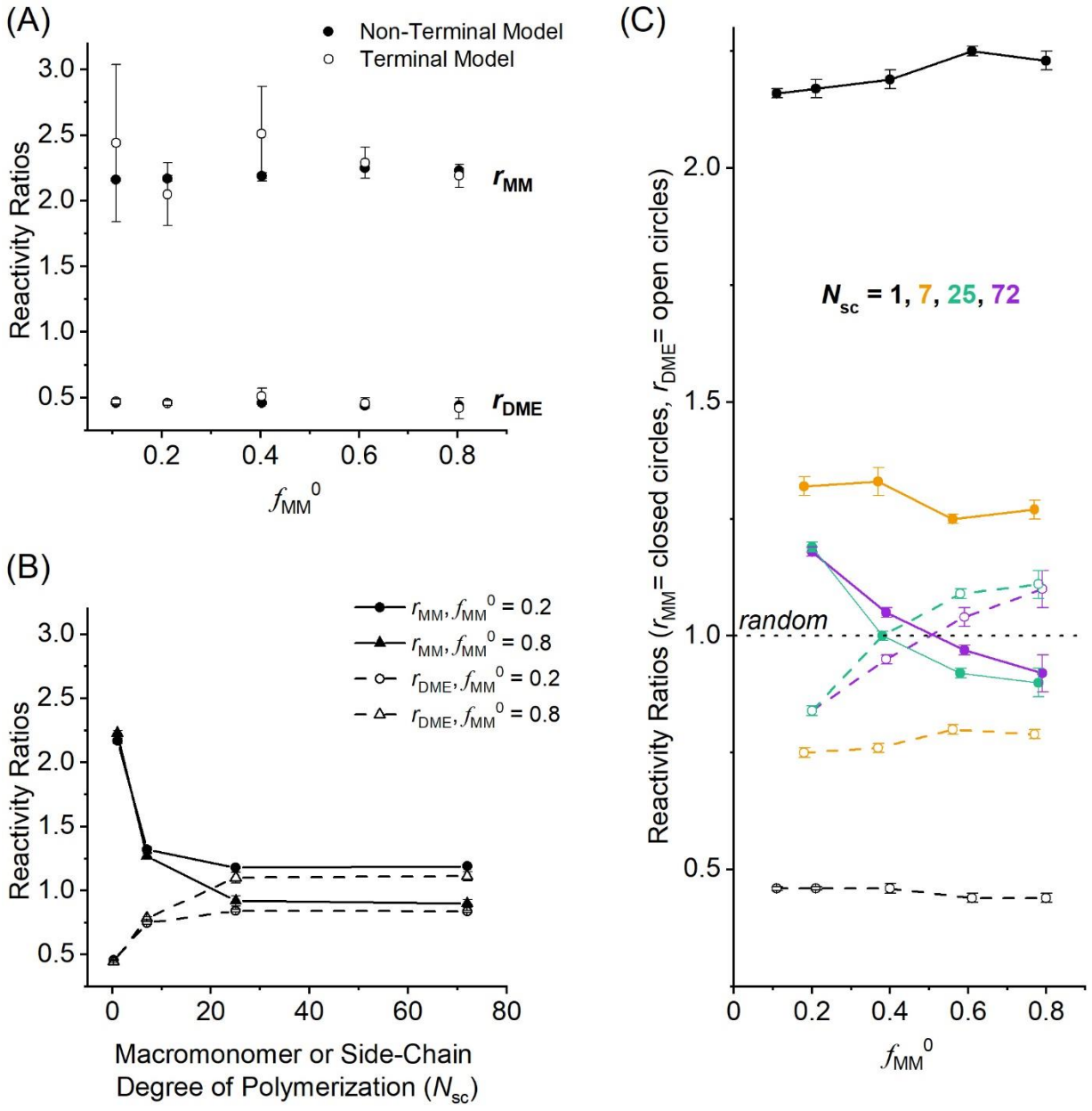

Figure 2. (A) Reactivity ratios derived from fits of the terminal and non-terminal models for copolymerization of the acetylated norbornene macromonomer ($N_{sc} \approx 1$) and dimethyl ester norbornene (DME) comonomer at various initial feed compositions. (B) Reactivity ratios of each comonomer as a function of N_{sc}, determined using a non-terminal model. Two different initial feed compositions are compared. (C) Non-terminal reactivity ratios of each comonomer as a function of f_{MM}^0, where the various colors correspond to copolymerizations using different N_{sc}. All error

bars correspond to the standard error of each fitting parameter, which is smaller than the data point in most cases.

A series of copolymerizations using a range of initial MM feed compositions (i.e., $0.1 \leq f_{MM}^0 \leq 0.8$) were studied. The resulting data in Figure 2A show that the reactivity ratios (r_{MM} and r_{DME}) from each model are within error of one another. Furthermore, r_{MM} is significantly greater than r_{DME} for all copolymerizations at $N_{sc} \approx 1$, and both are essentially independent of f_{MM}^0. The reactivity ratios suggest that at the monomeric limit ($N_{sc} \approx 1$), gradient copolymers are formed. Figure 2B and 2C show results from the non-terminal model, where the reactivity ratios are defined as $r_{MM} = k_{MM}/k_{DME} = 1/r_{DME}$. The model stipulates that the cross-propagation and self-propagation rate constants are equivalent and given as k_{MM} and k_{DME} for the MM and DME comonomer, respectively. Thus, each reactivity ratio is proportional to the reactivity of its respective monomer. The results in Figure 2B show that r_{MM} decreases and r_{DME} increases as N_{sc} increases. However, these quantities reach a plateau at large values of N_{sc}, where r_{MM} and r_{DME} are independent of N_{sc} and both are close to 1, consistent with a random copolymerization (defined as $r_{MM} = r_{DME} = 1$). For copolymerizations using macromonomers with $N_{sc} > 1$, fitting the data to the ML equation was not feasible since the equation becomes unstable as the reactivity ratios approach unity.[36] Figure 2B also shows that increasing f_{MM}^0 from 0.2 to 0.8 decreases r_{MM} and increases r_{DME} but only at larger values of N_{sc}. At low N_{sc}, the reactivity ratios are essentially independent of f_{MM}^0. This phenomenon can be seen clearly in Figure 2C, which presents the reactivity ratios as a function of f_{MM}^0 at all values of N_{sc} studied. Interestingly, at $N_{sc} = 25$ or 72, $r_{MM} > r_{DME}$ at low values of f_{MM}^0 and $r_{MM} < r_{DME}$ at high values of f_{MM}^0.

If a non-terminal model can be used to describe the copolymerization kinetics, a more-comprehensive terminal model should produce the same reactivity ratios. This is important to demonstrate, as a non-terminal model assumes that monomer reactivity does not depend on the composition of the growing chain. To our knowledge, the non-terminal model has only been used once for ROMP.[38] In this case, the ideality of the copolymerization and accuracy of the simulated

results were not rigorously proven, however. As seen in Figure 2A, both models fit the data consistently for reactivity ratios far from 1, which suggests the non-terminal model provides a sufficient description of the results. For copolymerizations that are near-random ($r_{MM} \approx r_{DME} \approx 1$), a limitation of the ML equation (terminal model) is that it becomes numerically unstable and produces large regression errors when fitting data – if a fit is possible. This difficulty arises because the ML equation is undefined when either of the reactivity ratios equal one (Equation S1.7). Here, the ML equation fails to fit the data while the BSL equations (non-terminal model) accurately describe the near-random copolymerization. Taken together, these observations support the applicability of a simpler non-terminal description of the data. Since the macromonomers with different values of N_{sc} all have the same reactive norbornene end-group and are copolymerized with the same comonomer, any change in the reactivity ratios, associated with changes to N_{sc} or z, must be due to steric effects. As N_{sc} increases, the steric hinderance imposed by the side-chains increasingly limits each comonomer's ability to incorporate into a growing chain (Figure 3).

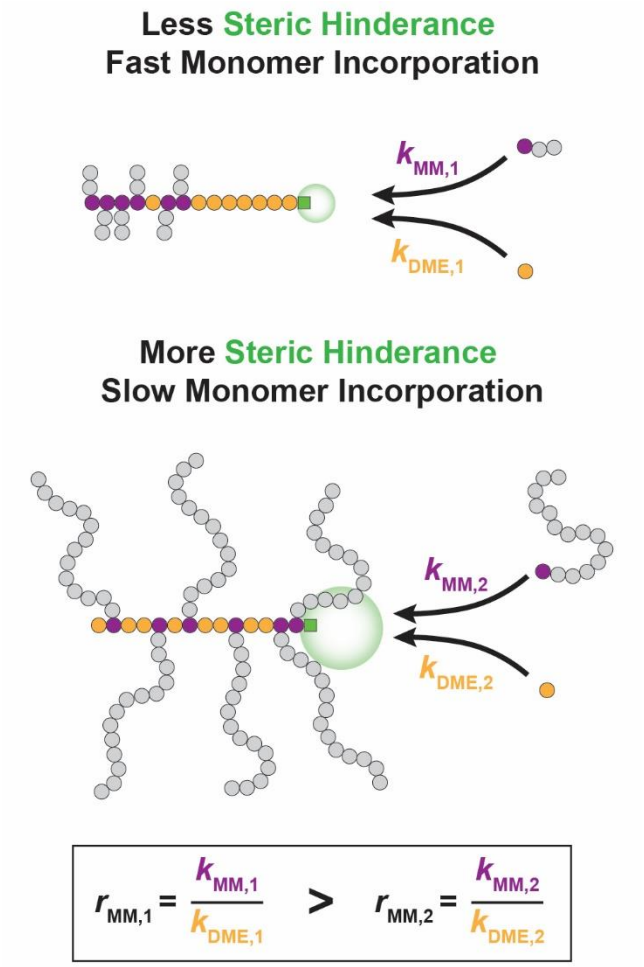

Figure 3. Schematic representation of a graft-through copolymerization. Increases to the side-chain degree of polymerization (N_{sc}) results in more steric hinderance (green circle) near the propagating chain-end (green square), which can slow monomer incorporation. This has a greater impact for the larger macromonomer, which results in a shift in the side-chain sequence distribution from gradient to near-random as N_{sc} increases for the comonomers used.

At first glance, the fact that steric hindrance of the copolymer backbone affects the reactivity ratios seems to disagree with the basis of a non-terminal copolymerization model where the identity of the repeat unit on the chain-end should not affect the incorporation of the next comonomer. This discrepancy is resolved by recognizing that macromonomer steric hindrance is not specific to the terminal repeat unit only but, instead, affects the copolymerization kinetics more generally.

The steric effect on reactivity ratios is more pronounced for the larger macromonomers (i.e., higher N_{sc} values), compared to the small dimethyl ester comonomer (DME). Because copolymerization is a *competitive process*, this unbalanced change in steric hinderance for each monomer results in opposing effects: the macromonomer incorporation becomes less favorable ($r_{MM} < 1$) with increasing N_{sc}, while the small comonomer reactivity ratio increases with $r_{MM} \times r_{DME} \approx 1$. However, the reactivity ratios approach near-constant values as N_{sc} becomes sufficiently large. This implies that increasing the side-chain size does not continuously increase its steric hinderance near the propagating center. This is expected since only the local environment surrounding a propagating chain-end will impact monomer incorporation. Side-chain steric bulk that is located further away from this region likely has a negligible impact (Figure 4) under reaction conditions that are not mass transport limited.

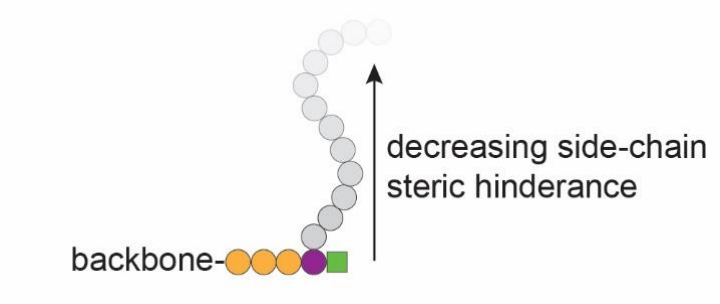

Figure 4. Side-chain repeat units (i.e., grey circles) located closest to the propagating chain-end (i.e., green square) will sterically impact monomer incorporation. Repeat units far away from the propagating chain-end will not have a steric impact. This causes the reactivity ratio dependence on N_{sc} to saturate as N_{sc} becomes large.

As a result, we observe a dependence of the reactivity ratio on the side-chain degree of polymerization up to $N_{sc} \lesssim 20$. This asymptotic behavior also has been reported for controlled radical[30] and anionic copolymerizations[25] of poly(methyl methacrylate) and polystyrene macromonomers, respectively, suggesting that the phenomenon is general to any graft-through copolymerization. The macromonomer composition likely impacts how quickly the asymptotic limit is reached as N_{sc} increases, which can be related to chain flexibility. For controlled radical

copolymerizations, Radke and Müller found the macromonomer reactivity to decrease as N_{sc} decreased.[30] This is contrary to what we observed, which suggests that the relationship between the macromonomer size and its reactivity at low N_{sc} depends on the polymerization method used.

As reported above, for almost all the copolymerizations presented here, r_{MM} is greater than r_{DME}. We believe this is caused by differences in the structure of the norbornene units on each monomer. Norbornene molecules with *exo,exo* stereochemistry (i.e., as in the macromonomer) polymerize faster than those with *endo,exo* stereochemistry (i.e., as in the DME comonomer) using G3 as the ROMP catalyst.[23,39] For sufficiently large values of N_{sc} the initial monomer feed composition can have a substantial impact on monomer reactivity. In this limit, r_{MM} decreases to a value that is less than r_{DME} (Figure 2B, C), despite the inherent differences in norbornene reactivity. It is unlikely that this finding is uniquely related to the rate laws governing ROMP,[40] as this dependence has been demonstrated for group transfer copolymerizations.[30] As mentioned previously, this directly conflicts with the terminal and non-terminal models, which predict the reactivity ratios to be independent of f_{MM}^0. The consistency of our results with those reported in the literature suggests that the phenomenon is general to copolymerizations involving a large macromonomer. Therefore, as the macromonomer size approaches the monomeric limit (i.e., $N_{sc} = 1$), the reactivity ratios should no longer depend on f_{MM}^0. The data we present supports this claim (Figure 2B) and clearly illustrate how the reactivity ratios change with f_{MM}^0 as N_{sc} is varied. Given the dilute reaction conditions used, this is unlikely to be due to changes in monomer diffusivity as f_{MM}^0 and N_{sc} increase. Instead, increasing f_{MM}^0 increases the number of side-chains per graft

polymer, which increases the probability of a side-chain being situated closer to the propagating chain-end (Figure 5).

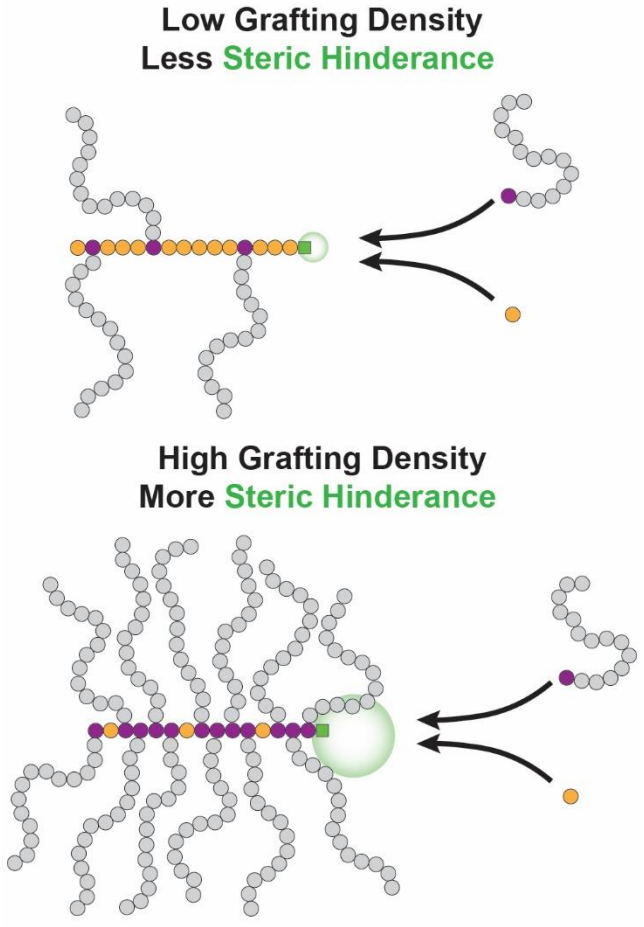

Figure 5. As the grafting density increases, the probability of side-chains existing near the propagating chain-end (i.e., green square) increases. This increases the probability of side-chains sterically hindering monomer incorporation, which has a measurable impact on the reactivity ratios.

Therefore, at high f_{MM}^{0} the probability of a side-chain sterically hindering an incoming monomer increases, causing r_{MM} to decrease.

The results demonstrated here should be applicable to graft-through copolymerizations in general, providing useful guidance for targeting specific side-chain distributions along a graft polymer backbone. Beyond a practical limit, the side-chain size has no substantial effect on the

monomer reactivity ratios (Figure 2B). In this limit, the impact of N_{sc} on material properties can be studied without inadvertently changing the desired graft distribution. For graft polymers with small side-chains (i.e., lower N_{sc} values), the reactivity ratios should be carefully monitored when N_{sc} is altered. In this limit, it could be advantageous to tune the incorporation rates (e.g., perfectly random) by changing N_{sc}, followed by chain-extension to produce longer side-chains. While changes to the initial feed composition do impact monomer reactivity ratios, this effect is relatively small and will not influence the reactivity ratios in a manner that would drastically affect the resulting graft polymer architecture (Figure 2C). All these findings are important for developing accurate structure-property relationships. The results from this study can be used as a guide for determining and characterizing the branch sequence in graft polymers synthesized via ROMP, using a simple non-terminal model of copolymerization. Coupling this approach to previous reports in the literature that describe comonomer selection for ROMP[22,23] creates a powerful tool for synthesizing graft polymers with well-defined side-chain distributions.

Associated Content

The Supporting Information is available free of charge at:

Experimental materials and methods, monomer characterization, and details regarding copolymerization kinetic data and analysis.

Author Information

Corresponding Authors:

Marc A. Hillmyer – Department of Chemistry, University of Minnesota, Minneapolis, MN, 55455-0431, United States; orcid.org/0000-0001-8255-3853; Email: hillmyer@umn.edu

Frank S. Bates – Department of Chemical Engineering and Materials Science, University of Minnesota, Minneapolis, MN, 55455-0132, United States; orcid.org/0000-0003-3977-1278; Email: bates001@umn.edu

Co-Authors:

Aristotelis Zografos – Department of Chemical Engineering and Materials Science, University of Minnesota, Minneapolis, MN, 55455-0132, United States; orcid.org/0000-0001-9612-091X

Nathaniel A. Lynd – McKetta Department of Chemical Engineering, The University of Texas at Austin, Austin, TX, 78712-1589, United States; orcid.org/0000-0003-3010-5068

Notes:

The authors declare no competing financial interest.

All primary data files are available free of charge at:

Acknowledgements

Support for this work was provided by the National Science Foundation (NSF) Center for Sustainable Polymers (CHE-1901635) at the University of Minnesota, as well as the NSF Graduate Research Fellowship Program (DGE-1839286). ^{1}H NMR experiments were conducted at the University of Minnesota Nuclear Magnetic Resonance Laboratory using an instrument that is supported by the Director, National Institutes of Health (S10OD011952). The content of this work is solely the responsibility of the authors and does not necessarily represent the official views of the National Institutes of Health. We thank Dr. Alice B. Chang, Dr. Michael G. Hyatt, Dr. Michael B. Sims, Dr. Christopher DeRosa and Dr. Lucie Fournier for helpful discussions and insight regarding polymer and monomer synthesis. We also acknowledge Dr. Alice B. Chang and Dr. Christopher DeRosa for providing the *exo,exo*-norbornene alcohol initiator used to synthesize the macromonomers. Lastly, we thank Dr. Letitia Yao, Dr. Michael B. Sims, and Claire Dingwell for their helpful insights regarding NMR characterization.

References

[1] Daniel, W. F. M.; Burdyńska, J.; Vatankhah-Varnoosfaderani, M.; Matyjaszewski, K.; Paturej, J.; Rubinstein, M.; Dobrynin, A. V.; Sheiko, S. S. Solvent-Free, Supersoft and Superelastic Bottlebrush Melts and Networks. *Nat. Mater.* **2016**, *15* (2), 183–189.

[2] Self, J. L.; Sample, C. S.; Levi, A. E.; Li, K.; Xie, R.; de Alaniz, J. R.; Bates, C. M. Dynamic Bottlebrush Polymer Networks: Self-Healing in Super-Soft Materials. *J. Am. Chem. Soc.* **2020**, *142* (16), 7567–7573.

[3] Zhang, J.; Schneiderman, D. K.; Li, T.; Hillmyer, M. A.; Bates, F. S. Design of Graft Block Polymer Thermoplastics. *Macromolecules* **2016**, *49* (23), 9108–9118.

[4] Abbasi, M.; Faust, L.; Wilhelm, M. Comb and Bottlebrush Polymers with Superior Rheological and Mechanical Properties. *Adv. Mater.* **2019**, *31* (26), 1806484.

[5] Shinoda, H.; Matyjaszewski, K.; Okrasa, L.; Mierzwa, M.; Pakula, T. Structural Control of Poly(Methyl Methacrylate)- g -Poly(Dimethylsiloxane) Copolymers Using Controlled Radical Polymerization: Effect of the Molecular Structure on Morphology and Mechanical Properties. *Macromolecules* **2003**, *36* (13), 4772–4778.

[6] Haugan, I. N.; Lee, B.; Maher, M. J.; Zografos, A.; Schibur, H. J.; Jones, S. D.; Hillmyer, M. A.; Bates, F. S. Physical Aging of Polylactide-Based Graft Block Polymers. *Macromolecules* **2019**, *52* (22), 8878–8894.

[7] Haugan, I. N.; Maher, M. J.; Chang, A. B.; Lin, T. P.; Grubbs, R. H.; Hillmyer, M. A.; Bates, F. S. Consequences of Grafting Density on the Linear Viscoelastic Behavior of Graft Polymers. *ACS Macro Lett.* **2018**, *7* (5), 525–530.

[8] Hu, M.; Xia, Y.; McKenna, G. B.; Kornfield, J. A.; Grubbs, R. H. Linear Rheological Response of a Series of Densely Branched Brush Polymers. *Macromolecules* **2011**, *44* (17), 6935–6943.

[9] Dalsin, S. J.; Hillmyer, M. A.; Bates, F. S. Linear Rheology of Polyolefin-Based Bottlebrush Polymers. *Macromolecules* **2015**, *48* (13), 4680–4691.

[10] Lentzakis, H.; Vlassopoulos, D.; Read, D. J.; Lee, H.; Chang, T.; Driva, P.; Hadjichristidis, N. Uniaxial Extensional Rheology of Well-Characterized Comb Polymers. *J. Rheol. (N. Y. N. Y).* **2013**, *57* (2), 605–625.

[11] Kempf, M.; Ahirwal, D.; Cziep, M.; Wilhelm, M. Synthesis and Linear and Nonlinear Melt Rheology of Well-Defined Comb Architectures of PS and PpMS with a Low and Controlled Degree of Long-Chain Branching. *Macromolecules* **2013**, *46* (12), 4978–4994.

[12] Abbasi, M.; Faust, L.; Riazi, K.; Wilhelm, M. Linear and Extensional Rheology of Model Branched Polystyrenes: From Loosely Grafted Combs to Bottlebrushes. *Macromolecules* **2017**, *50* (15), 5964–5977.

[13] Levi, A. E.; Lequieu, J.; Horne, J. D.; Bates, M. W.; Ren, J. M.; Delaney, K. T.; Fredrickson, G. H.; Bates, C. M. Miktoarm Stars via Grafting-Through Copolymerization: Self-Assembly and the Star-to-Bottlebrush Transition. *Macromolecules* **2019**, *52* (4), 1794–1802.

[14] Lin, T.-P.; Chang, A. B.; Luo, S.-X.; Chen, H.-Y.; Lee, B.; Grubbs, R. H. Effects of Grafting Density on Block Polymer Self-Assembly: From Linear to Bottlebrush. *ACS Nano* **2017**, *11* (11), 11632–11641.

[15] Maher, M. J.; Jones, S. D.; Zografos, A.; Xu, J.; Schibur, H. J.; Bates, F. S. The Order–Disorder Transition in Graft Block Copolymers. *Macromolecules* **2018**, *51* (1), 232–241.

[16] Karavolias, M. G.; Elder, J. B.; Ness, E. M.; Mahanthappa, M. K. Order-to-Disorder Transitions in Lamellar Melt Self-Assembled Core–Shell Bottlebrush Polymers. *ACS Macro Lett.* **2019**, *8* (12), 1617–1622.

[17] Morozova, S.; Schmidt, P. W.; Bates, F. S.; Lodge, T. P. Effect of Poly(Ethylene Glycol) Grafting Density on Methylcellulose Fibril Formation. *Macromolecules* **2018**, *51* (23), 9413–9421.

[18] Akar, I.; Keogh, R.; Blackman, L. D.; Foster, J. C.; Mathers, R. T.; O'Reilly, R. K. Grafting Density Governs the Thermoresponsive Behavior of P(OEGMA- Co -RMA) Statistical Copolymers. *ACS Macro Lett.* **2020**, *9* (8), 1149–1154.

[19] Paturej, J.; Sheiko, S. S.; Panyukov, S.; Rubinstein, M. Molecular Structure of Bottlebrush Polymers in Melts. *Sci. Adv.* **2016**, *2* (11), e1601478.

[20] Liang, H.; Morgan, B. J.; Xie, G.; Martinez, M. R.; Zhulina, E. B.; Matyjaszewski, K.; Sheiko, S. S.; Dobrynin, A. V. Universality of the Entanglement Plateau Modulus of Comb and Bottlebrush Polymer Melts. *Macromolecules* **2018**, *51* (23), 10028–10039.

[21] Liang, H.; Cao, Z.; Wang, Z.; Sheiko, S. S.; Dobrynin, A. V. Combs and Bottlebrushes in a Melt. *Macromolecules* **2017**, *50* (8), 3430–3437.

[22] Lin, T.-P.; Chang, A. B.; Chen, H.-Y.; Liberman-Martin, A. L.; Bates, C. M.; Voegtle, M. J.; Bauer, C. A.; Grubbs, R. H. Control of Grafting Density and Distribution in Graft Polymers by Living Ring-Opening Metathesis Copolymerization. *J. Am. Chem. Soc.* **2017**, *139* (10), 3896–3903.

[23] Chang, A. B.; Lin, T.-P.; Thompson, N. B.; Luo, S.-X.; Liberman-Martin, A. L.; Chen, H.-Y.; Lee, B.; Grubbs, R. H. Design, Synthesis, and Self-Assembly of Polymers with Tailored Graft Distributions. *J. Am. Chem. Soc.* **2017**, *139* (48), 17683–17693.

[24] Ren, N.; Yu, C.; Zhu, X. Topological Effect on Macromonomer Polymerization. *Macromolecules* **2021**, *54* (13), 6101–6108.

[25] Gnanou, Y.; Lutz, P. The Ability of Macromonomers to Copolymerize: A Critical Review with New Developments. *Die Makromol. Chemie* **1989**, *190* (3), 577–588.

[26] Ohno, S.; Matyjaszewski, K. Controlling Grafting Density and Side Chain Length in Poly(n-Butyl Acrylate) by ATRP Copolymerization of Macromonomers. *J. Polym. Sci. Part A Polym. Chem.* **2006**, *44* (19), 5454–5467.

[27] Roos, S. G.; Müller, A. H. E.; Matyjaszewski, K. Copolymerization of n -Butyl Acrylate with Methyl Methacrylate and PMMA Macromonomers: Comparison of Reactivity Ratios in Conventional and Atom Transfer Radical Copolymerization. *Macromolecules* **1999**, *32* (25), 8331–8335.

[28] Shinoda, H.; Miller, P. J.; Matyjaszewski, K. Improving the Structural Control of Graft Copolymers by Combining ATRP with the Macromonomer Method. *Macromolecules* **2001**, *34* (10), 3186–3194.

[29] Shinoda, H.; Matyjaszewski, K. Structural Control of Poly(Methyl Methacrylate)- g -Poly(Lactic Acid) Graft Copolymers by Atom Transfer Radical Polymerization (ATRP). *Macromolecules* **2001**, *34* (18), 6243–6248.

[30] Radke, W.; Müller, A. H. E. Copolymerization of Methacryloyl-Terminated PMMA Macromonomers with Methyl Methacrylate. *Makromol. Chemie. Macromol. Symp.* **1992**, *54–55* (1), 583–594.

[31] Walsh, D. J.; Guironnet, D. Macromolecules with Programmable Shape, Size, and Chemistry. *Proc. Natl. Acad. Sci.* **2019**, *116* (5), 1538–1542.

[32] Radzinski, S. C.; Foster, J. C.; Chapleski, R. C.; Troya, D.; Matson, J. B. Bottlebrush Polymer Synthesis by Ring-Opening Metathesis Polymerization: The Significance of the Anchor Group. *J. Am. Chem. Soc.* **2016**, *138* (22), 6998–7004.

[33] Percec, V.; Wang, J. H. The Influence of Total Monomers Concentration and Polymerization Solvent on the "Reactivity" of ω-(p-Vinylbenzyl Ether) Macromonomers of Poly(2,6-Dimethyl-1,4-Phenylene Oxide). *J. Polym. Sci. Part A Polym. Chem.* **1990**, *28* (5), 1059–1071.

[34] Beckingham, B. S.; Sanoja, G. E.; Lynd, N. A. Simple and Accurate Determination of Reactivity Ratios Using a Nonterminal Model of Chain Copolymerization. *Macromolecules* **2015**, *48* (19), 6922–6930.

[35] Meyer, V. E.; Lowry, G. G. Integral and Differential Binary Copolymerization Equations. *J. Polym. Sci. Part A Gen. Pap.* **1965**, *3* (8), 2843–2851.

[36] Lynd, N. A.; Ferrier, R. C.; Beckingham, B. S. Recommendation for Accurate Experimental Determination of Reactivity Ratios in Chain Copolymerization. *Macromolecules* **2019**, *52* (6), 2277–2285.

[37] Jaacks, V. A Novel Method of Determination of Reactivity Ratios in Binary and Ternary Copolymerizations. *Die Makromol. Chemie* **1972**, *161* (1), 161–172.

[38] Wang, H.; Onbulak, S.; Weigand, S.; Bates, F. S.; Hillmyer, M. A. Polyolefin Graft Copolymers through a Ring-Opening Metathesis Grafting through Approach. *Polym. Chem.* **2021**, *12* (14), 2075–2083.

[39] Wolf, W. J.; Lin, T.-P.; Grubbs, R. H. Examining the Effects of Monomer and Catalyst Structure on the Mechanism of Ruthenium-Catalyzed Ring-Opening Metathesis Polymerization. *J. Am. Chem. Soc.* **2019**, *141* (44), 17796–17808.

[40] Hyatt, M. G.; Walsh, D. J.; Lord, R. L.; Andino Martinez, J. G.; Guironnet, D. Mechanistic and Kinetic Studies of the Ring Opening Metathesis Polymerization of Norbornenyl Monomers by a Grubbs Third Generation Catalyst. *J. Am. Chem. Soc.* **2019**, *141* (44), 17918–17925. https://doi.org/10.1021/jacs.9b09752.